UCLA
UCLA Previously Published Works

Title
Solid-Liquid Hydrid Thermal Interfaces for Low-Contact Pressure Thermal Switching

Permalink
https://escholarship.org/uc/item/1fk4z0v9

Journal
Journal of Heat Transfer, 136

Authors
Ju, Y. Sungtaek
Jia, Yanbing

Publication Date
2014-06-16

Peer reviewed

eScholarship.org Powered by the California Digital Library
University of California

SOLID -LIQUID HYBRID THERMAL INTERFACES FOR LOW-CONTACT PRESSURE THERMAL SWITCHING

Y. Jia and Y. S. Ju[a]

Department of Mechanical and Aerospace Engineering

University of California,

420 Westwood Plaza, Los Angeles, CA 90095-1597, U.S.A.

[a)] corresponding author. email: just@seas.ucla.edu

Abstract

Switchable thermal interfaces allow controlled modulation of thermal conductance and are a key enabler of micro-devices and systems that require reconfigurable heat transfer paths. We report a solid-liquid hybrid thermal interface for reliable low-contact pressure (< 1 kPa) switching with on-state thermal contact resistance < 15 $\times 10^{-6}$ m^2K/W. Reduction in the thermal resistance of hybrid interfaces created through electroplating was evaluated using transient pulsed heating measurements and thermal time constant characterization. Compared with pure liquid-mediated interfaces and direct solid-solid contacts reported previously, the hybrid interface shows superior thermal performance under the same loading pressure while avoiding the use of liquid metals. The hybrid interface may be readily used with low-power electrostatic or Lorenz force-based actuators as part of integrated thermal micro-devices.

Key words: thermal switch, microscale heat transfer, waste heat harvesting, solid-state refrigeration

Nomenclature

C	thermal capacitance of the actuation plate, J/K
d	gap between the substrates, m
F_s	capillary force, N
R	thermal resistance of the hybrid interface, K/*W*
t	time after the actuation plate makes contact with the hot reservoir, s
T	temperature of the actuation plate, °C
T_i	initial temperature of the actuation plate, °C
T_r	temperature of the hot reservoir, °C
V	liquid volume, m^3
θ	apparent contact angle, °
τ	thermal time constant, s

Introduction

Switchable thermal interfaces allow controlled modulation of thermal conductance and are a key enabler of micro-devices and systems that require reconfigurable heat transfer paths or active thermal switching as integral parts of their functionalities. These include micro-bolometers with locally adjustable dynamic ranges, pulsed thermoelectric (TE) refrigeration where transient enhanced cooling is achieved by temporarily decoupling the TE elements from their cooling load, solid-state electrocaloric refrigeration and pyroelectric waste heat harvesting where a dielectric material must undergo thermodynamic cycles, and satellite thermal management [1–6].

Our recent studies [7,8] demonstrated liquid-based switchable thermal interfaces that can circumvent drawbacks of conventional and nano-engineered direct solid-solid contacts, including requirements of very large loading pressure [1] and various failure mechanisms such as fracture, cold welding, incomplete contact due to debris, and delamination of interfacial layers [9,10].

Further reduction in the actuation (switch-on) loading pressure, however, is needed before one may incorporate these interfaces into MEMS devices. Electrostatic or electromagnetic forces very often used in micro-devices are relatively weak at length scales of the order of 100 μm, which is necessary for reliable switching and high on/off ratios.

We now report an improved switchable thermal interface where an array of micromachined metal posts is embedded in a capillary confined liquid droplet to significantly enhance heat conduction in the on-state. Figure 1 schematically illustrates the solid-liquid hybrid interface design concept. This hybrid interface design allows us to achieve a low thermal resistance at much reduced loading pressure while avoiding the use of liquid metals [2], which either pose health and environmental hazard or oxidize rapidly in the ambient air.

Sample Preparation

The hybrid interface was prepared by electroplating Cu through a lithographically defined photoresist mold and forming an array of Cu microposts. Details of our process flows are discussed in [11] and will not be repeated here. Briefly, we first deposited a seed layer (30 nm Ti / 350 nm Cu / 30 nm Ti) on a silicon substrate using e-beam thermal evaporation (CHA Mark 40). We note that, although we used silicon substrates pre-coated with such a seed layer in the present work, the versatile electroplating approach can be readily adapted to any electrically conducting substrates to create the liquid-solid hybrid interfaces. We spin coated a negative photoresist (PR) layers on the substrate and lithographically patterned it to create an array of through-holes as a mold. We next removed the protective Ti layer and the native oxide layer formed on the seed layer under the through-holes using a diluted solution of hydrofluoric acid. The sample was then immersed in a commercial Cu electroplating bath and a low initial plating current density (~ 1 mA/cm^2) was applied to facilitate the formation of good electrical and mechanical contacts between the electrochemically deposited copper and the seed layer. Once electrodeposition was activated in all through-holes, the current density was increased (~ 7 mA/cm^2) to achieve higher deposition rates. After the completion of the electrodeposition, the sample was rinsed multiple times and the PR layer was stripped to expose the Cu micropost array.

Figure 2 shows the SEM image of microposts of diameter 100 μm, height 65 μm, and solid fraction (areal fraction of the microposts) 20% after the photoresist layer was removed. The microposts were confined within a circular region of diameter 6 mm (Fig. 1c). A hydrophobic Teflon layer was applied outside the region through contact printing. A droplet of water was next deposited on the hydrophilic region (Fig. 1d) to form a liquid-solid hybrid interface.

Mechanical Characteristics: Loading Pressure

One important characteristic of the switchable thermal interfaces is the force-gap relation, in particular, the maximum loading force required to balance the capillary forces and achieve the on-state where two surfaces defining the interface are pressed against each other until the liquid layer thickness and hence the interface thermal resistance reaches the targeted minimum value. In previous studies, we and others predicted such relations for liquid bridges using the virtual work model in conjunction with the surface energy minimization algorithm and validated them experimentally [7].

For the present liquid-based switchable interfaces, the in-plane liquid droplet diameter (> 6 mm) is much larger than the gap (~ 100 μm). The liquid meniscus can therefore be reasonably modeled using an arc approximation. One can then write an approximate analytic expression for the capillary force, which is the sum of the contributions from the Laplace pressure and the surface tension, as

$$F_s \approx 2\sigma\pi\sqrt{\frac{V}{\pi d}}\sin(\theta) + \sigma\left(\frac{2\cos(\theta)}{d^2}V - \sqrt{\frac{\pi V}{d}}\right)$$

Here, σ is the surface tension coefficient of the liquid-air interface, d is the gap between the substrates, θ is the apparent contact angle, and V is the liquid volume. For small gaps, the second term representing the Laplace pressure dominates over the first term representing the surface tension force. For a pinned liquid bridge, where the liquid contact area remains constant, the liquid volume V varies approximately in proportion to the gap d. As a result, the capillary force scales approximately as $F_s \sim V/d^2 \sim 1/d$.

For an interface thickness (or gap) of 75 μm, the corresponding loading pressure is only about 1 kPa for water despite its relatively high surface tension. We use de-ionized water in the present study because it allows the surfaces to be readily cleaned and reused. For practical applications, non-volatile liquids, such as ionic liquids with nearly zero vapor pressure, may be more suited to minimize or possibly eliminate a need for refilling the interfaces.

Thermal Resistance Characterization

To experimentally characterize the thermal resistance of our thermal interfaces, we used a thin-film serpentine heater lithographically patterned on one side of a silicon substrate. The other side of the substrate was coated with a layer Teflon to render it hydrophobic.

Figure 3a shows the experimental setup we used for the characterization of the thermal resistance of our interfaces. We applied a current pulse of a precisely defined amplitude to the serpentine heater and obtained temporal changes in its temperature by monitoring the temperature-dependent electrical resistance using a data acquisition system equipped with a 16-bit analog-to-digital converter. Each temporal temperature profile (Fig. 3b) was then analyzed using 3D transient finite element simulation to extract the thermal resistance across the interface.

Figure 4 shows the thermal resistance of the hybrid interface as a function of the interface thickness. The inverse of the slope of a linear fit to the thermal resistance versus thickness data is approximately 0.6 W/m K, which agrees with the thermal conductivity of liquid water. This result is consistent with the fact that the effective thermal resistance of the Cu micropost array (0.9×10^{-6} m^2K/W), calculated using the thermal conductivity of an electroplated Cu film, is negligible. The total thermal interface resistance is therefore dominated by that of the thin liquid overlayers sandwiched between the top plane of the microposts and the top substrate. The thermal

conductivity of the Cu film (350 W/m K) was obtained from the measured electrical resistivity using the Wiedemann-Franz law. At the same micropost height of 65 μm, micropost arrays of lower solid fractions, down to approximately 10%, may still provide sufficiently small thermal resistance (< 10 percent of the liquid overlayer resistance).

The measured thermal resistance of the present 75 μm-thick hybrid interface is 13×10^{-6} m^2K/W, which is equivalent to that of a 10 μm-thick pure (without microposts) liquid water layer. Since the capillary force is approximately inversely proportional to the interface thickness, we therefore can achieve as much as 7 fold reduction in the loading pressure necessary to achieve the same thermal resistance for this particular sample.

Thermal Time Constant Measurements

To further demonstrate the thermal performance benefit, we measured the thermal time constant of a thin plate that was made into a sudden contact with a hot reservoir through three different thermal interfaces: a direct solid-solid contact, a liquid thermal interface, and a liquid-solid hybrid thermal interface. The thin plate emulates a ferromagnetic actuation plate in previously reported thermomagnetic energy harvesters and thermal switches [12] and a thin-film pyroelectric or electrocaloric material for previously reported thermal-to-electric energy conversion and refrigeration devices [5,6].

An aluminum block with an embedded thermistor was used as a hot thermal reservoir. Its temperature was controlled by adjusting power input to a Peltier device attached on the bottom. Three silicon substrates, each incorporating one of the three different thermal interfaces, were mounted on the aluminum block using thermal grease.

We used a thin silicon actuation plate with a built-in thin-film resistance thermometer to monitor its temperature as a function of time after contact with the hot thermal reservoir. The plate was attached to a spring frame using epoxy dots of low thermal conductivity. The spring constant of the frame was pre-calibrated by hanging a set of reference weights and monitoring the resulting deflections. The spring frame itself was mounted on a motorized translation stage so that we could control and monitor the gap spacing/spring deflection using a high-speed digital camera.

For each experiment reported here, we maintained loading pressure to a target value of approximately 0.5 kPa (± 0.1 kPa) to ensure fair comparison among the three thermal interfaces. This loading pressure is of the order of the electrostatic pressure expected at a bias voltage of 100 V across a 100 μm-thick water layer.

Figure 5 shows the normalized temperature rise in the actuation plate as a function of time after contact for the three different thermal interfaces. As expected, the direct solid-solid contact requires the longest time for the plate to reach the reservoir temperature and hence has the largest thermal resistance. The solid-liquid hybrid interface outperforms the pure liquid interface even though the total interface thickness and hence the loading force remain the same.

Under the lumped capacitance model, the thermal time constant τ can be related to the thermal interface resistance:

$$\frac{T - T_i}{T_r - T_i} = 1 - \exp\left(-\frac{t}{RC}\right) = 1 - \exp\left(-\frac{t}{\tau}\right)$$

Here, T is the temperature of the actuation plate, T_r is the temperature of the hot reservoir, T_i is the initial temperature of the actuation plate, t is the time after contact with the hot reservoir, C is the thermal capacitance of the actuation plate, and R is the thermal interface resistance.

The thermal time constants extracted by analyzing the data using the lumped capacitance model are 350 ms, 135 ms, and 75 ms for the direct solid-solid contact, the liquid interface, and the hybrid interface, respectively. The latter two values compare reasonably well with the thermal time constants (150 ms and 70 ms) calculated using the independently measured thermal interface resistance values. Even for the relatively large gap used here, the hybrid interface offers almost 5-fold reduction compared with the direct solid-solid contact and almost 2-fold reduction compared with the pure liquid interface.

Summary and Conclusion

In summary, we successfully demonstrated a solid-liquid hybrid thermal interface for reliable low-contact pressure (< 1 kPa) switching with on-state thermal contact resistance < 15 $\times 10^{-6}$ m^2K/W. Compared with the liquid-mediated interface and the direct solid-solid contact, it shows superior thermal performance under the same loading pressure. Such interfaces may be readily used with low-power electrostatic or Lorenz force-based actuators as part of integrated thermal MEMS devices.

REFERENCES

[1] Song, W.-B., Sutton, M. S., and Talghader, J. J., 2002, "Thermal contact conductance of actuated interfaces," Appl. Phys. Lett., **81**(7), pp. 1216–1218.

[2] Cho, J., Richards, C., Bahr, D., Jiao, J., and Richards, R., 2008, "Evaluation of contacts for a MEMS thermal switch," J. Micromechanics Microengineering, **18**(10), p. 105012.

[3] Ghoshal, U., Ghoshal, S., McDowell, C., Shi, L., Cordes, S., and Farinelli, M., 2002, "Enhanced thermoelectric cooling at cold junction interfaces," Appl. Phys. Lett., **80**(16), pp. 3006–3008.

[4] Biter, W., Oh, S., and Hess, S., 2002, "Electrostatic switched radiator for space based thermal control," AIP Conf. Proc., **608**(1), pp. 73–80.

[5] Cha, G., and Ju, Y. S., 2013, "Pyroelectric Energy Harvesting using Liquid-Based Switchable Thermal Interfaces," Sensors Actuators Phys., **89**, pp. 100–107.

[6] Jia, Y., and Ju, Y. S., 2012, "A solid-state refrigerator based on the electrocaloric effect," Appl. Phys. Lett., **100**(24), p. 242901.

[7] Cha, G., and Ju, Y. S., 2009, "Reversible thermal interfaces based on microscale dielectric liquid layers," Appl. Phys. Lett., **94**, p. 211904.

[8] Jia, Y., Cha, G., and Ju, Y. S., 2012, "Switchable Thermal Interfaces Based on Discrete Liquid Droplets," Micromachines, **3**(1), pp. 10–20.

[9] Xu, J., and Fisher, T. S., 2006, "Enhancement of thermal interface materials with carbon nanotube arrays," Int. J. Heat Mass Transf., **49**(9–10), pp. 1658–1666.

[10] Zhao, Y., Tong, T., Delzeit, L., Kashani, A., Meyyappan, M., and Majumdar, A., 2006, "Interfacial energy and strength of multiwalled-carbon-nanotube-based dry adhesive," J. Vac. Sci. Technol. B Microelectron. Nanometer Struct., **24**(1), pp. 331–335.

[11] Nam, Y., Sharratt, S., Byon, C., Kim, S. J., and Ju, Y. S., 2010, “Fabrication and Characterization of the Capillary Performance of Superhydrophilic Cu Micropost Arrays,” J. Microelectromechanical Syst., **19**(3), pp. 581 –588.

[12] Bulgrin, K. E., Ju, Y. S., Carman, G. P., and Lavine, A. S., 2011, “An Investigation of a Tunable Magnetomechanical Thermal Switch,” J. Heat Transf., **133**(10), p. 101401.

Figure Caption

Figure 1: Solid-liquid hybrid interface: (a) off-state; (b) on-state; (c) top view of the mask pattern; (d) side view of the droplet after being deposited in the circular hydrophilic region incorporating microposts.

Figure 2: SEM of Cu microposts fabricated using the electrodeposition technique.

Figure 3: (a) Experimental setup for the thermal resistance characterization and (b) example temperature profiles obtained from measurements and FEM simulations.

Figure 4: Experimentally determined thermal resistance of the hybrid interface as a function of the liquid layer and hence the interface thickness.

Figure 5: Normalized temporal temperature profiles of the actuation plate in contact with the hot reservoir through the three different interfaces.

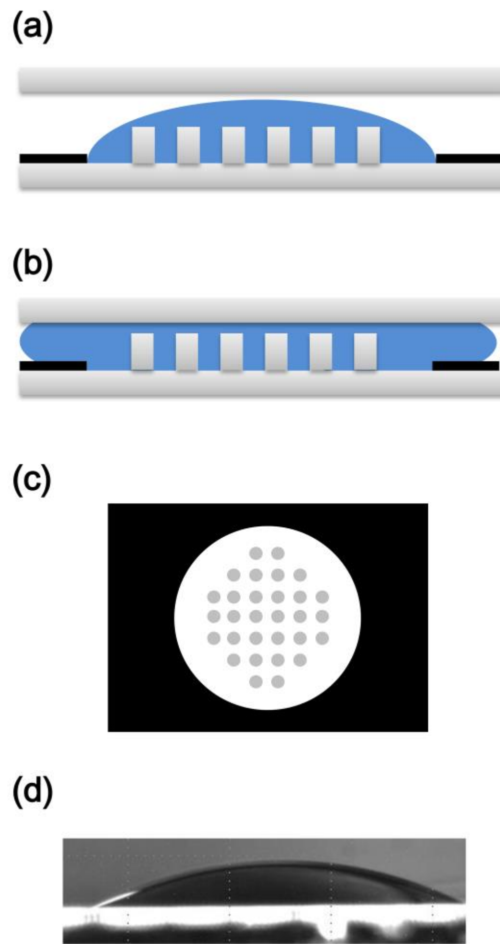

Figure 1 (color online only)

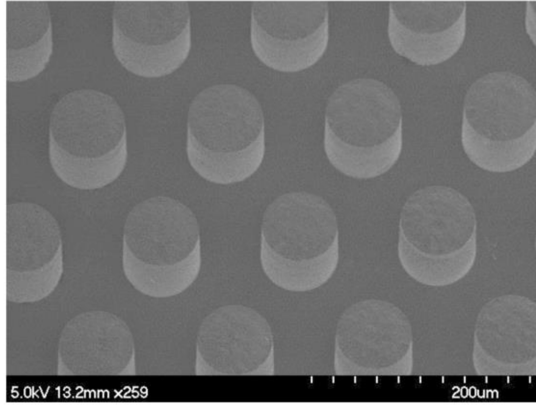

Figure 2

(a)

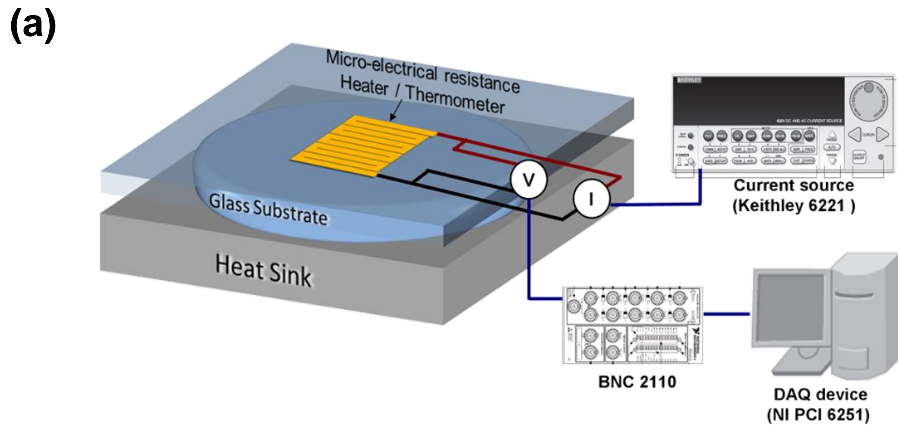

(b)

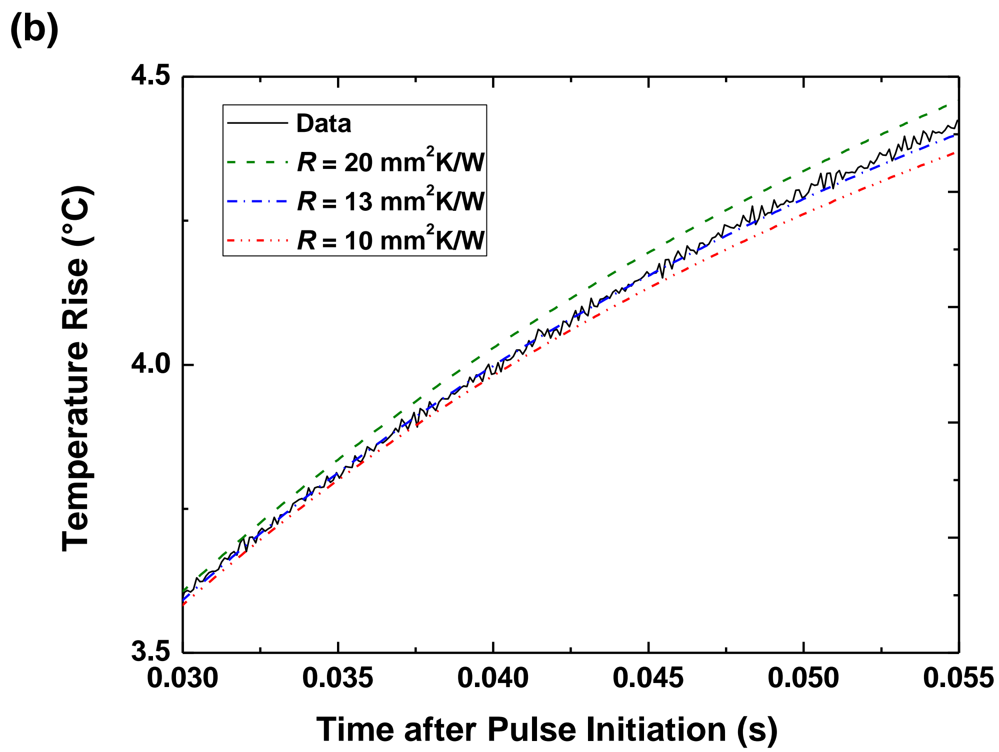

Figure 3 (color online only)

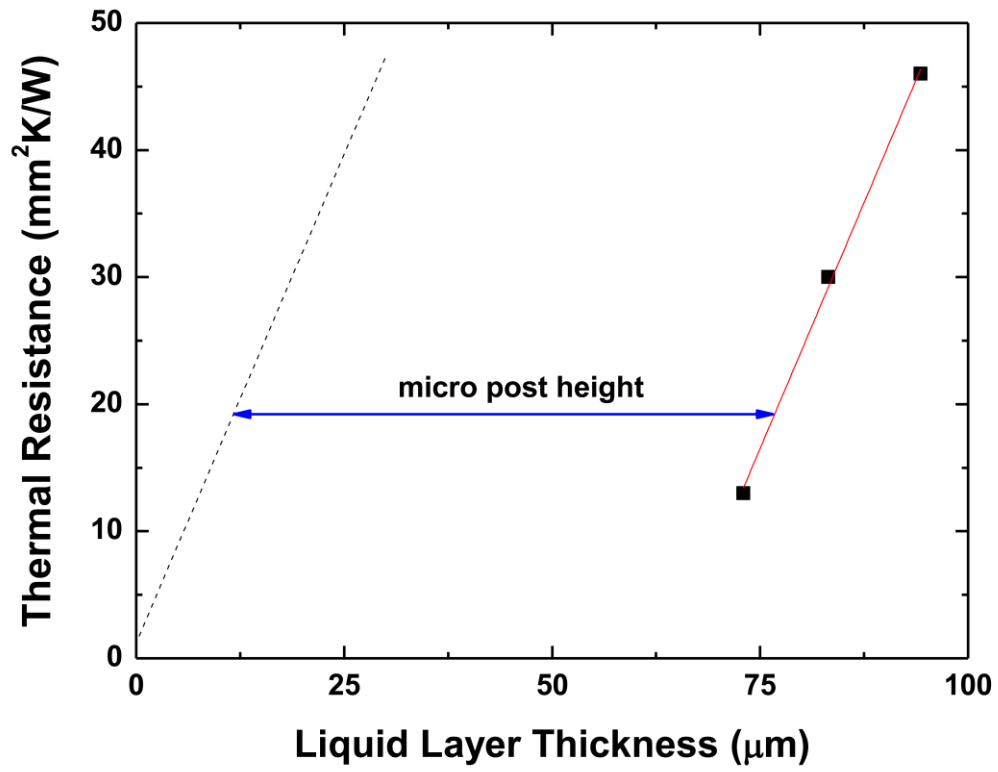

Figure 4 (color online only)

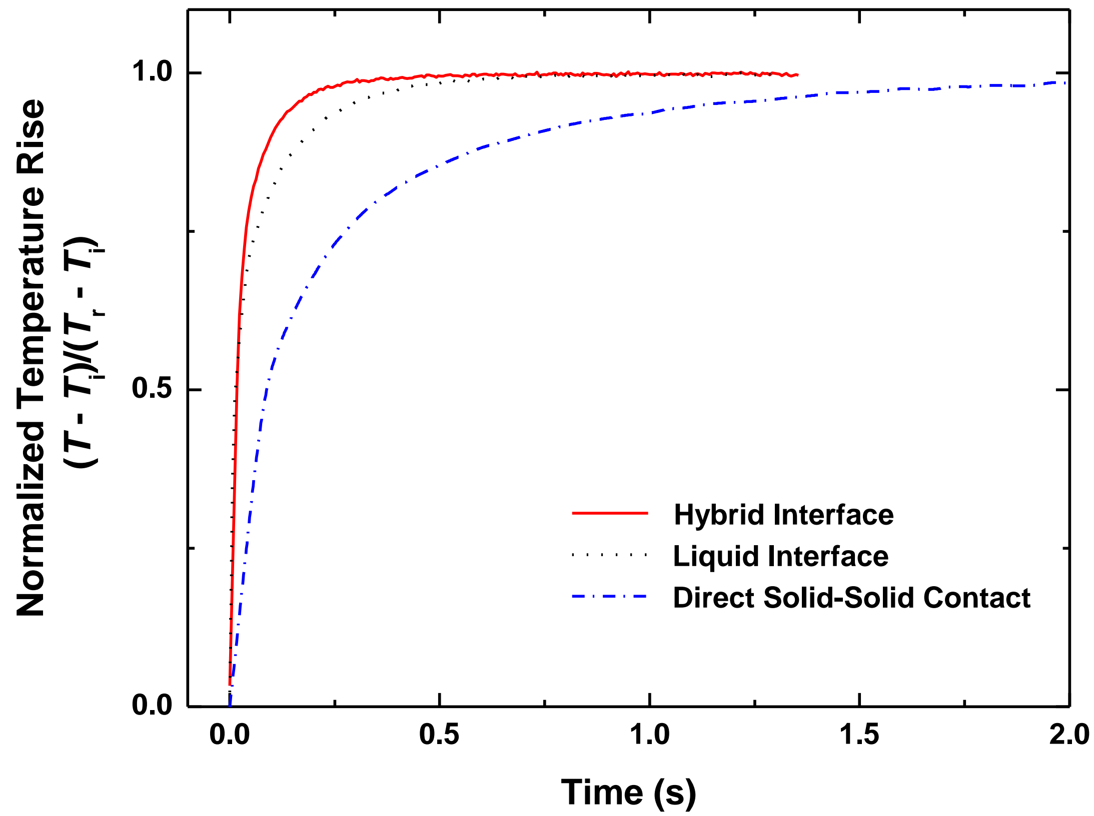

Figure 5 (color online only)